AIP | Journal of Applied Physics

Energy transfer from pyridine molecules towards europium cations contained in sub 5-nm Eu2O3 nanoparticles: Can a particle be an efficient multiple donor-acceptor system?

C. Truillet, F. Lux, T. Brichart, G. W. Lu, Q. H. Gong et al.

Citation: J. Appl. Phys. **114**, 114308 (2013); doi: 10.1063/1.4821428
View online: http://dx.doi.org/10.1063/1.4821428
View Table of Contents: http://jap.aip.org/resource/1/JAPIAU/v114/i11
Published by the AIP Publishing LLC.

Energy transfer from pyridine molecules towards europium cations contained in sub 5-nm Eu_2O_3 nanoparticles: Can a particle be an efficient multiple donor-acceptor system?

C. Truillet,[1] F. Lux,[1] T. Brichart,[1] G. W. Lu,[2] Q. H. Gong,[2] P. Perriat,[3] M. Martini,[1,a)] and O. Tillement[1]

[1]*Institut Lumière Matière, UMR 5306 CNRS, Université Claude Bernard, Villeurbanne 69622, France*
[2]*State Key Laboratory for Mesoscopic Physics, Department of Physics, Peking University, Beijing 100871, China*
[3]*MATEIS, UMR 5510 CNRS, INSA de Lyon, Villeurbanne 69661, France*

(Received 19 May 2013; accepted 2 September 2013; published online 18 September 2013)

Sensitized Eu_2O_3 nanoparticles coated by polysiloxane have been prepared using a polyol method. Further grafting of pyridine molecules on particles surface enhances 400-times the emission of the Eu^{3+} cations. The sensitizing effect of the pyridine molecules that transfer a part of their excitation towards Eu^{3+} has been studied by systematic excitation and emission measurements. All of the de-excitation pathway rates involved in the emission processes of these nanoparticles were determined. In particular, the transfer efficiency which was found independent of the number of sensitizers per particle is equal to 0.13 ± 0.01, a value quite satisfying taking into account that the donors and the acceptors are separated by a polysiloxane spacer of 0.4 nm. Furthermore this *multiple* donor-acceptor system has been modeled in order to deduce the average transfer efficiency as a function of the *single* donor-acceptor transfer rate. The theoretical modeling is in complete coherence with the experiments performed on a series of samples varying the thickness of the polysiloxane shell, i.e., the spacing distance between the donors and the acceptors. All these results illustrate the interest of using such structures in applications requiring ultrasensitive detection. © *2013 AIP Publishing LLC*. [http://dx.doi.org/10.1063/1.4821428]

I. INTRODUCTION

Fluorescence detection techniques have been undoubtedly become the most suitable way to monitor the spatio-temporal modifications of biological processes. An accurate analysis of molecular binding, association, conformational change, diffusion, and catalysis—imposed via an extensive network of cascade and feedback mechanisms—requires in-vivo cellular imaging and in-vitro assays techniques whose detections at spatial and temporal scales must be consistent with the times and distances characteristic of the biological phenomena studied. In this scenario, while (i) the electron microscopy provides near molecular-level spatial resolution but prevents dynamic imaging and (ii) positron emission tomography, magnetic resonance imaging, and optical coherence tomography provide real-time readout without discerning details smaller than 1 mm, 0.1 mm, and 0.01 mm, respectively, super resolution fluorescence techniques have been progressing quickly.[1] Indeed, techniques like Stimulated Emission Depletion (STED), fluorescence photo-activation localization microscopy (FPALM), or stochastic optical reconstruction microscopy (STORM) integrate (i) the advantages of a high spatial resolution (breaking the diffraction limit)[2–4] and (ii) a real-time readout of seconds, allowing dynamic and minimally invasive cell imaging experiments.[5] Recently, STED microscopy has achieved 20 nm-resolution in the focal plane and 45 nm-resolution in all three dimensions, but this accuracy could be further enhanced by the use of still brighter fluorescent tracers.

The real-time nanoscale localization of the individual fluorescent spots is given by the number of emission photons over the fluorescence background noise. The maximization of the S/N fluorescence ratio increases the spatial resolution of imaging.[6] Rare earth (RE) ions based phosphorescent structures are attractive substitutes for the more commonly used organic fluorophores such as Green fluorescent proteins, fluoresceins, or cyanines[7–9] because of (i) their long-life photon emission that overcomes the organic autofluorescence of the background and (ii) their large Stokes shift.[10–12] Dedicated and automated time-resolved luminescence-based platforms as DELFIA® and FIAgen™ have been developed and commercialized in the past decade.[13] For instance, the FIAgen™ platform has been applied to conventional heterogeneous microwell formats for immunoassays and membrane- or gel-based nucleic acid hybridization assays, in order to detect a wide variety of analytes with a low detection limit (10^{-11} mol/l).[14]

The design of lanthanide-based platforms as efficient detection tool has to take into account primarily the weak luminescence of rare earth ions compared to the organic extrinsic probes. The poor conversion of incident light to emission signal is mainly due to the low molar extinction coefficient of lanthanides (due to forbidden *f-f* transitions) rather than to their specific quantum yield. As reported in literature,[11,15–17] the observed absorption cross-section of lanthanides ε_{Ln} is lower than $3\ M^{-1}\ cm^{-1}$ (e.g., $1.8\ M^{-1}\ cm^{-1}$ for Eu^{3+}) whereas it lies in the range of $50\,000\ M^{-1}\ cm^{-1}$ (e.g., fluorescein molecules

a)Author to whom correspondence should be addressed. Electronic mail: matteo.martini@univ-lyon1.fr. Tel.: +33 4 27 46 57 26. Fax: +33 4 72 43 12 33.

$80\,000\ M^{-1}\,cm^{-1}$) for organic dyes. Since the improvements of quantum yield values that are already superior to 0.1 are limited to 1, it is clear that the emission efficiency of rare earth tracers has to go through the increase of ε_{Ln}. The works of Weissman in 1942 (about the salicylaldehyde and P-diketonate complexes of lanthanides)[18] opened the way to the lanthanide emission sensitization research. Since then, rare earths have not been treated as single entities (as performed for organic dyes) but as phosphorescence systems composed of an activator (the lanthanide ion), a host lattice (the ion surrounding material), and sometimes an organic antenna.[19]

The development of new lanthanide-based platforms for time-resolved imaging techniques has been dominated by the polydentate complexes systems.[20] Several works, notably the ones of Selvin[21] and Wong,[22] have intensely investigated the choice of the appropriate ligand for an efficient sensitization of rare earths evaluating the binding strength of the ligands, the absence of high-frequency vibrational modes, and the closeness of ligand excited states to the ones of lanthanides. Aromatic pyridine ligands have been widely considered as the best candidates for the enhancing of RE luminescence with a hypothetical increment of overall absorption cross-section more than 10 000-fold.[19] In the majority of the cases, the discussion only concerned single activator–antenna coupling (donor/acceptor D/A pairs). Nevertheless, the deficiency of a systematic exploration of multi-donor or multi-acceptor configurations is paradoxical,[23] considering the extreme variety of the multiple D/A configurations that are encountered in biology: D/A homogeneous solutions, D/A lipid bilayers, or even D/A double stranded DNAs.[24–26]

In this framework ruled by the molecular coordination systems,[27,28] we would like to evaluate the efficiency of nanostructure-based sensitized configurations as potentially substitute of organic ligands. The choice of RE hybrid nano-oxide particles as topic of this paper is dictated by two main reasons. First, such nanoparticles were recently proven to be efficient contrast agents in several *in vitro* and *in vivo* tracing applications,[29,30] and second, the optical mechanisms taking place in sensitized nanoparticles have been still unknown. Pyridine-grafted core/shell particles (core = europium oxide, shell = polysiloxane matrix) have been synthesized and systematically characterized. The core/shell architecture (Figure 1) constitutes a multiple donor/acceptor (D/A) system in which each pyridine molecule acts as a donor (D) and the europium cations of the core as acceptors (A).

Such D/A systems are generally characterized by the emission efficiency η, which is defined as the fraction of the excited donors that allow a radiative de-excitation of the acceptors. η depends (i) on the efficiency of the excitation transfer between the donor and the acceptor η_T and (ii) on the quantum yield of the lanthanide acceptor Φ_A; it is then given by[21]

$$\eta = \eta_T \Phi_A. \tag{1}$$

In Eq. (1), η_T is equal to

$$\eta_T = \frac{k_T}{k_{rD} + k_{nrD} + k_T}, \tag{2}$$

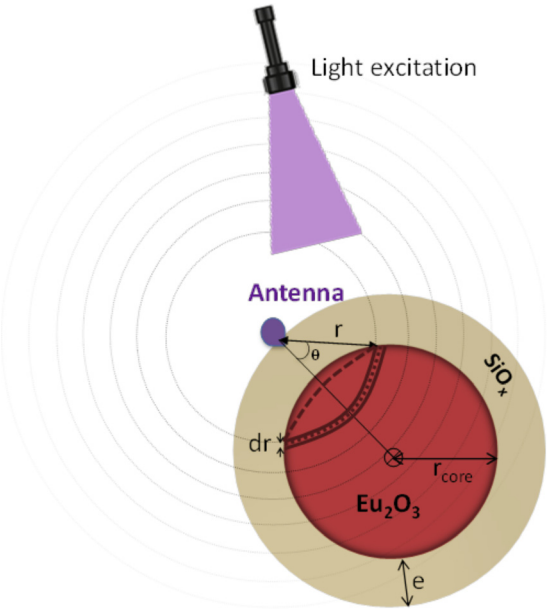

FIG. 1. Nanoparticle scheme with definition of the variables involved in calculations.

where k_T is the average transfer rate of excitation energy from the pyridine molecules (D) to the Eu^{3+} cations (A) and k_{rD} and k_{nrD} are, respectively, the radiative and non-radiative decay rates of the pyridine molecules.

The lanthanide quantum yield is defined itself as the fraction of the excited acceptors that decay by the radiative pathway. It is equal to

$$\Phi_A = \frac{k_{rA}}{k_{rA} + k_{nrA}}, \tag{3}$$

where k_{rA} and k_{nrA} are the radiative and non-radiative decay rates of the europium cations.

In this paper, we measure (i) the emission efficiency η of such a system and (ii) all the de-excitation pathway rates k_T, k_{rD}, k_{nrD}, k_{rA}, k_{nrA} involved in the sensitization processes. With the aim of progressing in the systematic comprehension of multiple D/A systems, (iii) the average transfer properties of the whole particle will be correlated to those of the single D/A pairs. Moreover, we proposed an original modeling of transfer mechanism that considers the possibility that one pyridine could transfer the energy to several europium cations of core. We prove that the energy transfer between the pyridine donors and the Eu^{3+} acceptors leads to an enhancement of the lanthanide emission equal to 400 compared with the emission of pure acceptors (coated oxide cores). The results open the way to the use of pyridine-sensitized lanthanide oxides as innovative platforms for ultra-sensitive fluorescence techniques.

II. EXPERIMENTAL

A. Chemicals

Europium chloride hexahydrate ($EuCl_3{\cdot}6H_2O$, 99%), sodium hydroxide (NaOH, 99.99%), tetraethyl orthosilicate

($Si(OC_2H_5)_4$, TEOS, 98%), aminopropyl triethoxysilane ($H_2N(CH_2)_3$-$Si(OC_2H_5)_3$, APTES, 99%), triethylamine (TEA, 99.5%), dimethyl sulfoxide (DMSO, 99.5%), 2,6-Pyridinedicarboxylic acid were purchased from Sigma-Aldrich Chemicals. Diethylene glycol (DEG, 99%) was purchased from SDS Carlo Erba. Absolut ethanol (99.9%) was purchased from VWR. Only Elga Purelab Ultra water ($\rho > 18\,M\Omega$) was used for the preparation of the aqueous solutions.

B. Synthesis

1. Eu_2O_3 core synthesis

Nanostructured Eu_2O_3 cores have been synthesized according to the polyol method under Ar atmosphere.[31,32] 1.1 g of chloride precursors ($EuCl_3{\cdot}6H_2O$) were first dissolved in 100 ml of DEG. The 24-h progressive addition of sodium hydroxide solution (400 mg NaOH, 1 ml water, 99 ml DEG) at room temperature followed by a thermal annealing at 450 K for 4 h allows the formation of monodisperse Eu_2O_3 oxide nanoparticles. The presence of DEG (35.7 cP at 300 K) helps to prevent aggregation between nanoparticles whereas the excess of NaOH (over-stoichiometric conditions) limits the fraction of unreacted Eu^{3+} ions.[33] The stability of europium cores in DEG is ensured for several months. The obtained solution was diluted to get a final concentration of 1.5 mM in europium.

2. Polysiloxane coating of Eu_2O_3 cores

A polysiloxane shell growth was induced by hydrolysis-condensation of siloxane precursors in the presence of the oxide cores at fixed 40 °C. The addition of APTES-TEOS precursors mixture (60:40 molar ratio) in the presence of a basic catalyst solution (DEG with 0.1 M of TEA and 10 M of water) induces a progressive polysiloxane coating of the Eu_2O_3 cores. Each addition step—corresponding to 84 μl of APTES, 54 μl of TEOS, and 204 μl of the catalyst solution in 400 ml of the solution containing the europium oxide particles—leads to the formation of approximately 34 μl of polysiloxane matrix (considering a sol-gel yield of 100% and polysiloxane density equal to 1.6 g/cm^3). Among this quantity elaborated (34 μl), only a limited part (comprised between 33% and 42%) participates in the formation of polysiloxane shell, the remaining polysiloxane clusters being eliminated during further purification steps.[34] Between single additions, the solution was left under stirring for 24 h. The number of single additions (between 1 and 4) determines the thickness of the final silica coating.

3. 2,6-pyridinedicarboxylic acid labeling

The covalent grafting of antennas onto the Eu_2O_3 core–SiOx shell is ensured by an amide bond between the carboxyl groups of the 2,6-pyridinedicarboxylic acid molecules and the amino groups relative to APTES molecules. To obtain the suitable number of antennas per particle, the corresponding amount of 2,6-pyridinedicarboxylic acid molecules was directly added to the solution containing the core/shell nanoparticles. The solution was stirred during 24 h under Ar atmosphere to complete the reaction.

C. Characterization

1. TEM characterization

Detailed structural and morphological information were obtained by TEM analysis, using a JEOL 2010F microscope operating at 200 kV. The samples were prepared by evaporation of a 10 μl drop of colloidal solution onto a carbon grid (200 mesh) at room temperature.

2. Dynamic light scattering measurements (DLS)

Direct measurement of the particles size distribution was performed using a Zetasizer Nano ZS from Malvern Instruments (He-Ne laser 633 nm, 5 mW, with 173° NIBS detector and narrow band filter). Samples were measured using DEG as dispersant medium. DLS gives the main parameters related to size distribution, i.e., the average size and the mean standard deviation, which characterize the size homogeneity of the sample studied.

3. UV-vis spectroscopy studies

UV-vis extinction spectra were recorded at room temperature using a Cary 50 spectrometer from Agilent Technologies. Quartz cells (Hellma Analytics) with an optical length of 10 mm were used for all optical measurements. The extinction band was measured in the 210–800 nm range. Samples were diluted in absolute ethanol (final europium concentration in ethanol equal to 150 μM) to avoid dissolution of the oxide cores.[30]

4. Luminescence spectra

The excitation, emission spectra (in both steady-state and time-resolved configuration), and lifetime decays were measured at room temperature using a Cary Eclipse spectrophotometer developed by Agilent Technologies (75 kW Xenon flash lamp, Czerny-Turner monochromators, Δpulse = 2 μs, 800 V PM detector). Samples were diluted in absolute ethanol (europium concentration equal to 1.5 μM) to get an optical density <0.10 (at the excitation wavelength of 270 nm), in order to prevent the reabsorption. The excitation wavelength was adjusted to 270 nm, which corresponds to the HOMO-LUMO absorption transition of pyridine molecules.[35]

5. Inductively coupled plasma-atomic emission spectrometry (ICP-AES) analysis

Determination of the europium and silicon content in samples was performed by ICP-AES analysis (with a Varian 710-ES spectrometer). Before measurements, samples of colloidal solution were dissolved in concentrated nitric acid, heated for 3 h at 80 °C, and left one night at RT. The samples were then diluted with water until the nitric acid concentration in water reached 5%.

III. RESULTS AND DISCUSSION

A. Preparation and characterization of the samples studied

1. Core synthesis

Two different series of Eu_2O_3 core–polysiloxane shell–antenna coated nanoparticles were prepared for systematic luminescence assays. The variation of only one parameter per series helps the optimization of the particle structure and the comprehension of its optical properties and the phosphorescence efficiency. Both series use the same Eu_2O_3 core (Figure 1): (i) in one case, it was just varied the amount of pyridine molecules per particle (fixing the pyridine–Eu_2O_3 core distance) whereas (ii) in the second case it was varied the polysiloxane thickness of the particle (fixing the amount of pyridine molecules per particle).

The powder characterization after DEG removal (X-ray diffraction, nitrogen adsorption isotherm) is unfeasible because of the presence of ligand is essential to avoid any transformation from the oxide to the hydroxide. High-resolution transmission electron microscopy (HRTEM) was then performed on colloids to evidence the crystallization of the nanosized cores via the characteristic lattice fringes of europium oxide. These latter appear above the background caused by the polysiloxane shell and the carbon grid. In agreement with the optical data,[34] the Fast Fourier Transform (FFT) of the images taken confirmed the expected body centered cubic structure of Eu_2O_3 (space group Ia3).[30] The statistical analysis of particle population—made from several TEM micrographs—displays a Gaussian size distribution of around 3.6 ± 0.2 nm with a standard deviation equal to 0.6 ± 0.1 nm (Figure 2). Each Eu_2O_3 core of 3.6 nm (the diameter) contains about 670 europium atoms (calculations considered the Eu_2O_3 density of 7.42 g/cm^3). DLS assays corroborated the presence of a monodisperse particles population with a hydrodynamic diameter of 3.7 ± 0.1 nm (mean standard deviation of 0.7 ± 0.05 nm). According to the definition of the hydrodynamic diameter, the DLS values obtained are in a good correlation with the results of TEM assays. Furthermore, a positive skewness value in both histograms implies that the population considered contains a greater proportion of large cores, but this distribution asymmetry does not affect further luminescence analysis.

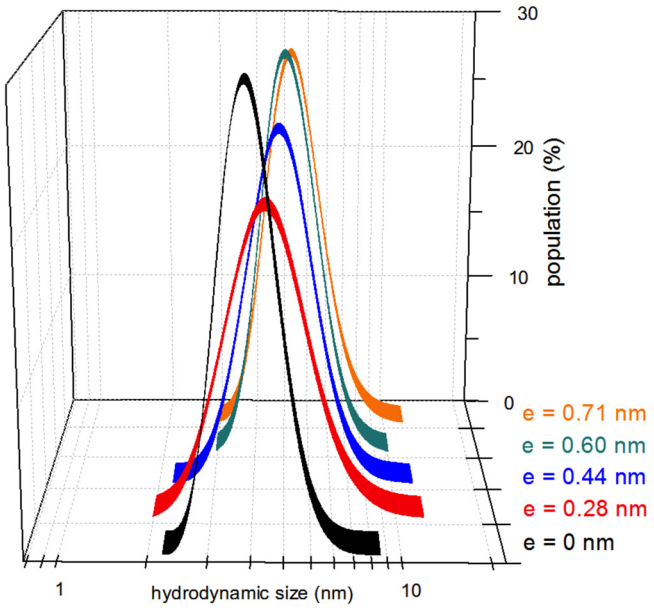

FIG. 2. Hydrodynamic size distribution of the particles with different polysiloxane coating thicknesses by DLS measurements.

2. Shell synthesis

The progressive addition of polysiloxane coating increases the final size of nanoparticles without significant modification of the skewness (DLS measurements). The hydrodynamic diameters of the core/shell (Eu_2O_3/polysiloxane) nanoparticles increase from 3.7 ± 0.1 nm (simple oxide core) to 4.2 ± 0.1 (msd 1.2 ± 0.05 nm), 4.5 ± 0.1 (msd 1.1 ± 0.05 nm), 4.9 ± 0.1 (msd 0.9 ± 0.05 nm), and 5.1 ± 0.1 (msd 1.1 ± 0.05 nm), depending on the silica precursors amount used. These values—in perfect agreement with the quantity of silica presents in the particles—confirm the formation of the polysiloxane coating of the cores (see Ref. 34 which summarizes the correlation between the size measured by DLS and the size calculated from the yield of polysiloxane coating). Moreover, optical measurements indicate that (i) this shell formed should be uniform and (ii) the polysiloxane encapsulation does not alter the structure of the oxide phase.[34] Indeed, as observed from the optical spectra the unchanged magnetic dipole transition intensity ($^5D_0 \rightarrow {}^7F_1$) after coating corroborates the core preservation. The slight increase of peak intensity is due to the diminution of the non-radiative de-excitation rate as a consequence of a decrease of surface hydroxyl quenchers. The growth of proportion between the intensities of the $^5D_0 \rightarrow {}^7F_2$ forced electric dipole transition (that is very sensitive to site-symmetry) and the $^5D_0 \rightarrow {}^7F_1$ band illustrates the modification of the europium surroundings by the polysiloxane layer. This variation ascertains the preservation of the bcc oxide phase since any transformation to hydroxide should decrease the ratio. EDX analyses (energy dispersive x-ray spectroscopy) performed with a $10\,\text{nm} \times 10\,\text{nm}$ electron-probe evidenced the presence of both europium and silicon elements in the expected proportions. Unfortunately, the insufficient contrast between the sub-nanometric polysiloxane shell and the carbon background of TEM grid prevents any size analysis of the series by electron microscopy. Polysiloxane thickness of 2 nm becomes visible in TEM only for cores larger than 5 nm.[33]

3. Pyridine grafting

The covalent grafting of antennas onto the surface of the Eu_2O_3/polysiloxane particles is ensured by the presence of available amino-group sites distributed within the polysiloxane matrix. Considering the specific case of particles with a polysiloxane shell thickness of 0.4 nm (the first series), the APTES precursors introduced correspond to 800 potential anchorage sites. The progressive addition of pyridine molecules does not affect the colloidal stability until the nominal value of 800 molecules per particle, above which the solution becomes turbid and the particles flocculate in a few hours. The nominal value of 800 does not mean that all of

the pyridine molecules introduced are grafted onto the particle but gives an estimation of the possible number of linked pyridines. Indeed, after purification steps—performed by ultrafiltration 5 kDa PES (polyethersulfone) membranes (purification rate higher than 10^2)—the waste fractional volume shows the presence of unreacted pyridine molecules. Absorption analysis of supernatant waste reveals that the fraction of pyridines grafted to the pyridine introduced *n* is closed to 1 till the threshold of 450. Over this value, the *n*-450 antenna introduced are unreacted and without purification free in solution.

B. Evidence of a Förster energy transfer from pyridine molecules toward europium cations

It is widely proven that the lanthanide's surrounding is fundamental for the enhancement of luminescence emission. We expect that the hybrid systems studied here consisting of pyridine-grafted particles containing Eu_2O_3 represent an efficient way to sensitize the emission signal of the Eu^{3+} activator centers.[36] On one hand, the host lattice (i.e., the oxide structure) offers a rigid platform that influences the emission transitions of the Eu^{3+} luminescence centers. On the other hand, the vicinity of pyridine molecule allows a controlled antenna effect between the organic molecules and the lanthanide cations. The estimation of each contribution (i.e., the host lattice and the antenna effect) to Eu^{3+} sensitization can be given by the analysis of the excitation spectra of three colloidal samples specifically prepared. These samples consist of (i) uncoated oxide cores (Eu_2O_3), (ii) polysiloxane coated Eu_2O_3 cores ($Eu_2O_3@SiO_x$), and (iii) polysiloxane coated and pyridine-grafted Eu_2O_3 cores ($Eu_2O_3@SiO_x@$pyridine). For the three samples, the final concentration of Eu_2O_3 core was fixed to 1.5 μM in europium, and—where present—the thickness of the coating was equal to 0.4 nm. The average number of pyridine molecules per particle is equal to 2.6, and it corresponds to a D/A ratio of 1/250.

The results of excitation assays are summarized in Figure 3. Regarding the $^5D_0 \rightarrow {}^7F_2$ emission transition (peak centered at 615 nm), several excitation bands appear in the VUV–UV range, but we only focused the discussion in the 220–400 nm energy window. The narrow peak at 395 nm—due to the direct excitation of europium ions (Ref. 37)—was taken as reference for the normalization of the luminescence intensities. This is experimentally justified since the intensity found for this peak is, at less than 10%, the same for the three samples studied. The high-energy excitation bands ($\lambda < 300$ nm) are due (i) to the Dexter energy transfer[38] from the host lattice and (ii) in the presence of pyridine molecules, to the Forster energy transfer[39] arising from the organic antenna. As expected, both Eu_2O_3 and $Eu_2O_3@SiO_x$ samples display a broadband situated between 220 and 290 nm. According to the Jorgensen spin pairing energy theory, this band is assigned to the charge transfer (CT) transitions occurring between the oxide scaffold and the europium cations (Eu^{3+}-O^{2-} transitions).[40,41] Indeed, this very broad absorption band, which is mainly vibronic in character,[42,43] concerns the transfer of valence electrons ($2p^6$ of O^{2-}) from the matrix toward the unoccupied orbitals 4f of the metallic cation, and it can be modeled by exchange processes as argued by Dexter in 1953.[38] It is noticeable that the presence of a polysiloxane coating significantly affects the excitation spectra with an overall increase in the CT energy band.[44] These spectral modifications mirror the strong dependence of the CT on the electronegativity of the surrounding, the electron affinity of the metal ions, and the ligand–metal distance.[45,46]

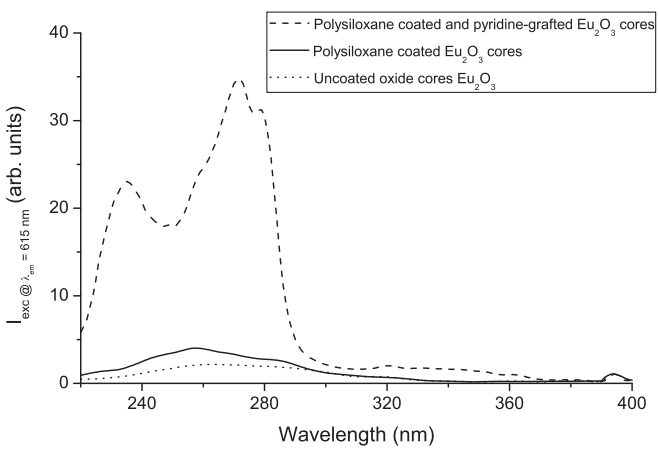

FIG. 3. Excitation spectrum monitored at 615 nm for uncoated Eu_2O_3 cores, polysiloxane coated Eu_2O_3 cores, and polysiloxane coated Eu_2O_3 cores grafted by pyridine molecules. The curves are normalized using the peak at 395 nm. The energy transfer related to the HOMO-LUMO transition bands of the pyridine molecules (Förster transfer of excitation) overcomes the one related to the host lattice (Dexter transfer of charge).

Furthermore, as seen in Figure 3, the lighting up of europium cores can still be boosted by the addition of pyridine molecules. Even for a donor-acceptor ratio as small as 1/250, the sensitizing effect due to the presence of organic antenna is found 20 times more important than the one originating from the host lattice. The consequent appearance in Figure 3 of an intense peak centered at 270 nm indicates the efficient repopulation of the excited states of the europium atoms by the electrons transferred from the dipicolinic acid molecules.[22] The broad and asymmetric absorption band around 37 100 cm^{-1} is assigned to a combination of $n \rightarrow \pi^*$ and $\pi \rightarrow \pi^*$ transitions of pyridine molecules (HOMO-LUMO transitions).[35,47,48] According to Kohn-Sham orbital theory, the HOMO and the next lowest occupied orbital (SHOMO) in pyridine molecules correspond to nonbonding (or poorly bonding) π orbitals that are approximately located in the pyridine plane and centered on the terminal carboxamide moieties. On the other hand, the LUMO orbitals correspond to π-antibonding orbitals perpendicular to the aromatic ring and centered on the pyridine ring (Figure 4).

As widely argued in literature, the overall antenna effect involves a multistep mechanism between the two components of a single donor-acceptor pair.[49] Although the internal mechanism of the transfer does not represent the object of this paper, a short description of these steps can be listed. Briefly (i) UV light is first collected by the singlet antenna-centered states $1\pi\pi^*$. Normally dipole transitions between pure singlet and pure triplet states $3\pi\pi^*$ are rigorously forbidden on account of the orthogonality of the spin-wave functions.[50] However through the intervention of spin-orbit coupling, (ii) inter-combinations between nominal singlet and triplet states are rendered possible. Finally, (iii) it is

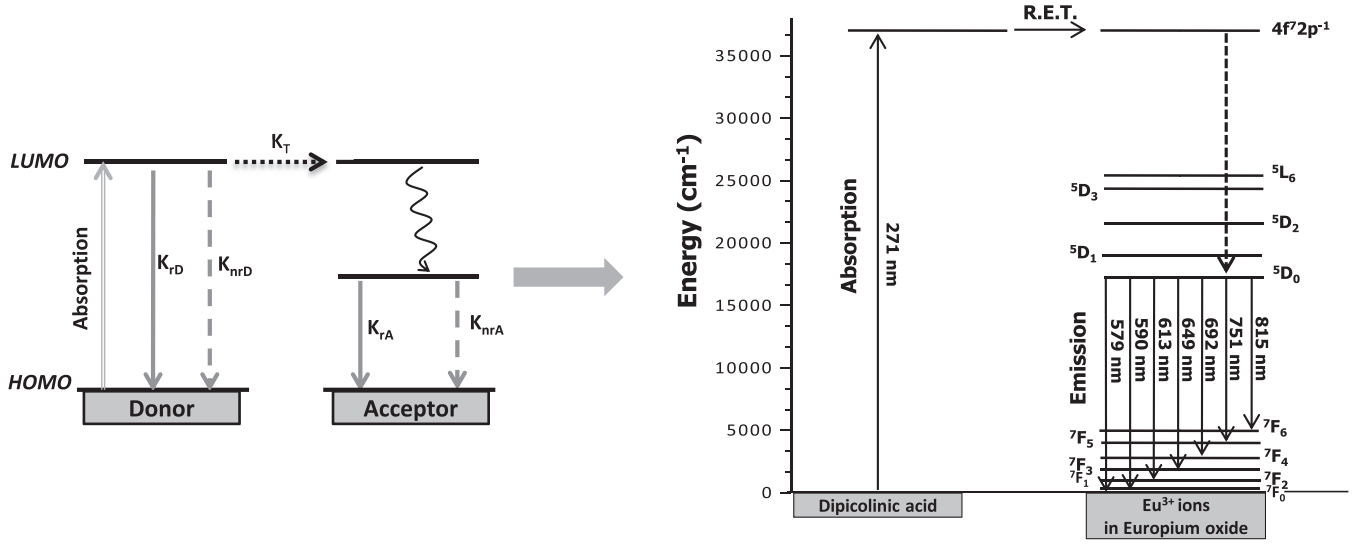

FIG. 4. Jablonski's diagram of the europium level energies under sensitized excitation. Inset: definition of the optical parameters involved in the emission processes.

generally accepted that the energy transfer from ligand to Eu^{3+} ions occurs from the lowest triplet state energy level of the pyridine (27 050 cm^{-1}) to the close resonance level of the Eu^{3+} ion (25 500 cm^{-1}).[19] This non-radiative energy transfer is confirmed by the unchanged position of the pyridine emission spectra in absence and presence of Eu^{3+} acceptors.[34] It is evident that the extension of energy transfer mechanisms from the case of single donor–acceptor pairs to the case of multiple D/A pair integrated in nanometric samples has to pass through a carefully analysis of the nanoparticle structure (Figure 4).

C. Systematic determination of the de-excitation rates in D/A pyridinated core/shells particles. Study of samples varying the number of pyridine molecules per particle

In a first series of samples composed of the same core/shell structure (0.4 nm polysiloxane coating 3.7 nm Eu_2O_3 cores), the number of pyridine molecules introduced per particle was increased from 2.6 to 800 (corresponding to a D/A ratio varying from 1/250 to 1.2). The emission efficiency (defined in Eq. (1)) of the multiple D/A system can be simply evaluated using the William's comparative method.[51] The η value is given by

$$\eta = \eta_{D/A} = \Phi_{ref} \frac{abs_{ref}}{abs_{D/A}} \frac{I_{emD/A}}{I_{emref}} \frac{I_{0ref}}{I_{0D/A}} \frac{{n_{D/A}}^2}{{n_{ref}}^2}. \quad (4)$$

In this equation, *abs* is the absorbance value (for particles smaller than 10 nm, the scattering of UV-Vis light can be neglected), I_{em} is the emission intensity, I_0 is the intensity of the incoming light, and n is the average refractive index of the solvent. Subscripts *ref* and *D/A* refer to the reference (with a known Φ) and to the test (with unknown η) samples, respectively. Using this formula, the absolute emission efficiency η of the D/A system can be simply extracted from the donor absorption and the acceptor emission spectra by comparison with those of a reference sample. The fluorescein molecule—chosen as reference sample—has a quantum yield of 0.92.

1. Measurements of donor absorbance

In the absence of particles scattering, the extinction spectrum of the solutions containing the pyridine-grafted particles coincides with the absorption one. All solutions have the same concentration of particles (135 particles per μm^3 that correspond to 150 μM in europium). All the absorption spectra display a peak centered at 270 nm, where its absorbance is proportional to the pyridine content per particle (Figure 5(a)). The absorbance values measured at 270 nm increase linearly from 0.008 to 2.5 for a number of molecules per particle n varying from 2.6 to 800. Applying the Lambert-Beer law to the experimental data, we found a molar extinction coefficient of pyridine equal to 8 630 $M^{-1}\,cm^{-1}$ (or in terms absorption cross section $3.3 \times 10^{-17}\,cm^2$).

2. Measurements of acceptor emission

The emission intensities of Eu^{3+} ions from the core were measured in high-diluted solution in order to exclude any inner filter effect, even if in the europium oxide the reabsorption is negligible because of its large Stokes shift. All the solutions were studied at the same concentration of particles (29 particles per μm^3 or 1.5 μM in europium). As reported in Figure 5(b), the emission signal of lanthanide nanoparticles (integrating the whole emission bands from 550 nm to 650 nm under 270 nm excitation) increases proportionally with the number of pyridine molecules per particle till the experimental value of 400 and then remained almost stable. The breaking of linearity in emission intensity is consistent with the maximal number of pyridine molecules that can be grafted onto the particles surface (equal to 450 pyridine per particle) as described in Sec. III A. Therefore, the n - 450 free molecules are unable to transfer their excitation to the europium cations because of their large distance from the oxide core.

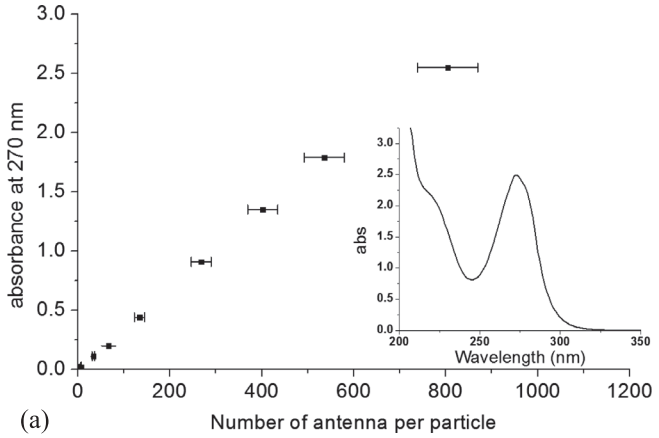

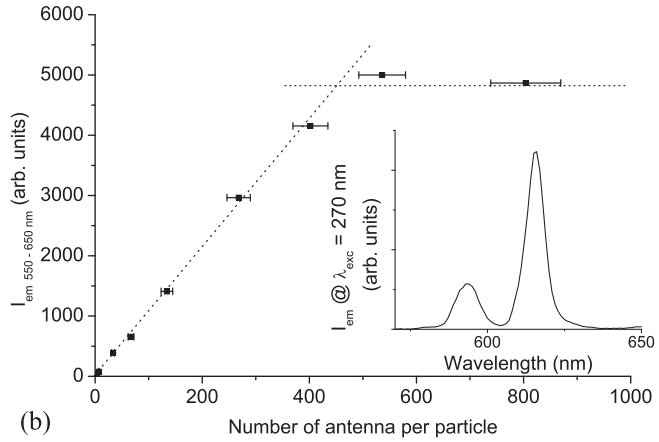

FIG. 5. (a) Absorbance values at 271 nm; (inset) extinction spectrum of polysiloxane coated Eu_2O_3 cores grafted by pyridine molecules. (b) Emission intensities integrated in the range 550–650 nm under 270 nm pulse excitation of polysiloxane coated Eu_2O_3 cores grafted by pyridine molecules with different D/A ratio. Inset: characteristic emission spectrum of the samples studied.

3. Determination of the emission efficiency

Figure 6 and Table I summarize the values of η obtained by the application of William's equation (Eq. (4)) for the different content of pyridine introduced. As expected, the n value of 450 represents the edge between two zones of the graph.

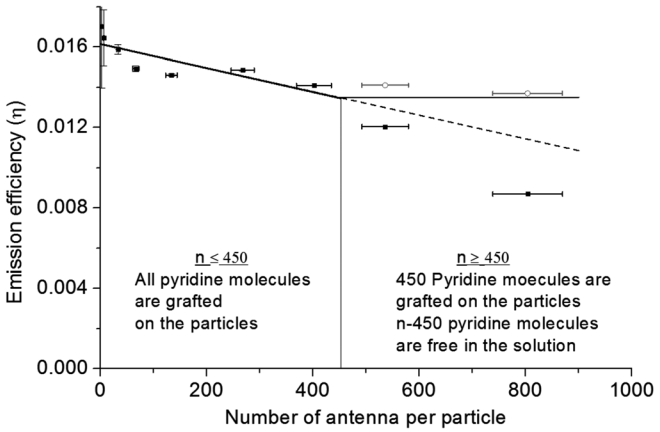

FIG. 6. Emission efficiency over the D/A ratio (or the number of pyridine molecules per particle) for Eu_2O_3 cores coated by a polysiloxane shell with a thickness of 0.3 nm.

When $n < 450$, the emission efficiency slightly decreases with the number of pyridine per particle (about 15% for the increasing of n from 2.6 to 450). Table I shows that the decrease of η is mainly due to the decrease of Φ_A. As consequence, regardless of the number of pyridine molecules introduced, the value of transfer efficiency η_T (defined in Eq. (2)) is approximately a constant (0.14 ± 0.02). This value is lower but still comparable to the one calculated by Selvin in single D/A coordinating systems (0.45–0.69).[21] When $n > 450$, the uncorrected emission efficiency values (square dots in Figure 6) calculated directly by the William's equation dramatically reduce of 50% due to the breaking of linearity of acceptor emission. The hollow spheres dots indicate the corrected values considering that only 450 molecules grafted onto the particles surface participate in the D/A energy transfer.

4. Estimation of all de-excitation pathway rates involved in the sensitization process

The complete description of the D/A system requires the knowledge of the radiative and non-radiative de-excitation rates of the pyridine molecules (k_{rD}, k_{nrD}), those of the europium cations (k_{rA}, k_{nrA}), and the average transfer rate (k_T)

TABLE I. Parameters of samples studied. η is the emission efficiency, η_T is the transfer efficiency, Φ_A the quantum yield of the lanthanide, R_0 the Förster distance, D/A the donor/acceptor molar ratio, $\langle d \rangle$ is the R^6-weighted distance between each antenna and all acceptors.

D/A	Antenna per particle	Silica thickness (nm)	$\langle d \rangle$ (nm)	R_0 (Å)	η	ϕ_A	η_T	k_{rD} (ns^{-1})	k_{nrD} (ns^{-1})	k_T (ns^{-1})	k_{rA} (ms^{-1})	k_{nrA} (ms^{-1})	lifetime (ms)
0.0040	2.68	0.44	1.5	89	0.015	0.16	0.12	0.05	1.2	0.14	0.21	1.12	0.75
0.0100	6.7	0.44	1.5	89	0.016	0.15	0.14	0.05	1.2	0.14	0.21	1.16	0.73
0.0500	33.5	0.44	1.5	89	0.016	0.15	0.13	0.05	1.2	0.14	0.21	1.20	0.71
0.1000	67	0.44	1.5	89	0.015	0.15	0.12	0.05	1.2	0.14	0.21	1.22	0.70
0.2000	134	0.44	1.5	89	0.015	0.15	0.12	0.05	1.2	0.14	0.21	1.22	0.70
0.4000	268	0.44	1.5	89	0.015	0.14	0.13	0.05	1.2	0.14	0.21	1.33	0.65
0.6000	402	0.44	1.5	89	0.016	0.13	0.14	0.05	1.2	0.14	0.21	1.38	0.63
0.8000	534	0.44	1.5	89	0.013	0.13	0.12	0.05	1.2	0.14	0.21	1.38	0.63
1.2000	804	0.44	1.5	89	0.013	0.13	0.12	0.05	1.2	0.14	0.21	1.38	0.63
0.0040	2.68	0.28	1.2	89	0.031	0.16	0.24	0.05	1.2	0.39	0.21	1.12	0.75
0.0040	2.68	0.60	1.9	89	0.006	0.16	0.046	0.05	1.2	0.06	0.21	1.12	0.75
0.0040	2.68	0.71	2.1	89	0.004	0.16	0.029	0.05	1.2	0.037	0.21	1.12	0.75

from the organic molecules to the lanthanide cations. The values of k_{rA} and k_{nrA} can be simply determined by the europium quantum yield measurements Φ_A and by their lifetime τ_A using an inverse function of Eq. (3).[52]

To measure the europium lifetime,[53] the samples were excited by δ-function that is repeated every 30 ms until 100 000 counts are obtained. From the decay curves—almost perfectly mono-exponential trends—the lifetime values were extracted and listed in Table I. As seen for the quantum yield values Φ_A, the acceptor lifetime value slightly decreases with the number of pyridine molecules n introduced due to an increase in k_{nrA} with n. While the radiative decay rate is not affected by a change in the ligand population (k_{rA} equal to 0.21 ms^{-1} regardless of n), k_{nrA} value goes up from 1.12 ms^{-1} (for $n = 2.6$) to 1.38 ms^{-1} (for $n = 400$) and remains stable for $n > 450$. The absolute value of both k_{rA} and k_{nrA} of series is consistent with results obtained for *naked* europium oxide cores (published elsewhere[28]). This asymptotic trend of k_{nrA} confirms that the excess of pyridine molecules free in solution has no effect upon the optical properties of the europium cations. The variation of k_{nrA} for $n < 450$ is probably due to the increase in the number of hydroxyl group quenchers closed to the luminescent centers that act as trap for light.[44,54] Indeed, although the polysiloxane coating shields the oxide core from the solvent effects, the increasing amount of pyridine molecules could alter the morphology of the shell and favors the migration of hydroxyl quenchers to the surface core.

From the donor's point of view, the constant value of transfer efficiency η_T regardless of the number of pyridine molecules guides the determination of the rates k_{rD}, k_{nrD}, and k_T using Eq. (2). Both k_T and k_{rD} are expected to be independent of the n value since the average donor-acceptor distance and the photonic mode density (PMD) remaining unchanged whatever the number of donors. Only the k_{nrD} value is expected to increase with the number of donors because of (i) the reduced inter-pyridine distance and (ii) the presence of traps for light (defective forms of pyridine) that increases the probability for a homo-transfer toward traps. However, the constant value of η_T, k_{rD}, and k_T with n implies that k_{nrD} must be a constant as well. Certainly the absence of defective pyridine molecules reduces the donor self-quenching. As a consequence, k_{rD} and k_{nrD} remain the same than those for isolated pyridine molecules. They are respectively equal to 0.05 ms^{-1} and 1.2 ms^{-1} ($\tau_D = 0.8$ ns, $\Phi_D = 0.04$).[55] By Eq. (2), the average transfer rate of donor for 0.44 nm-polysiloxane shell is equal to 0.14 ms^{-1}.

D. Determination of the parameters involved in the individual transfer rate occurring between each donor and acceptor of the D/A system. Study of samples varying the thickness of the polysiloxane shell

Considering a single D/A pair, the transfer rate value $k_T^0(r)$ depends on the distance r between the donor and the acceptor, as reported by Förster[39]

$$k_T^0(r) = \frac{1}{\tau_D}\left(\frac{R_0}{r}\right)^6, \tag{5}$$

where τ_D is the lifetime of the donor in absence of acceptor and R_0, the distance between the donor and the acceptor at which the transfer efficiency is 50%. For systems that involve several acceptors and donors, k_T (introduced by Eq. (2)) is the averaging of the $k_T^0(r)$ values over all the D/A couples of each nanoparticle.[56] In this section, k_T and η_T will be expressed as a function of the corresponding individual properties $(k_T^0(r), \eta_T^0(r))$ between each donor-acceptor pair. Calculations suppose that (i) the pyridine donors are lying on the particle surface at the same distance e from the core, (ii) the number of europium acceptors in the excited state is small compared with that in the ground state, (iii) the distances between the donor and the acceptors do not change during the excited state lifetime of the donor, and (iv) R_0 is the same for all the donor-acceptor pairs. Under these conditions, the averaging values are given by

$$k_T = \frac{1}{n_A}\int_{V_{core}} k_T^0(r)\sigma_A^V dV = \frac{1}{V_{core}}\int_{V_{core}} k_T^0(r)dV, \tag{6}$$

$$\eta_T = \frac{1}{n_A}\int_{V_{core}} \frac{k_T^0(r)}{k_{rD}+k_{nrD}+k_T^0(r)}\sigma_A^V dV = \frac{1}{V_{core}}\int_{V_{core}} \frac{k_T^0(r)}{k_{rD}+k_{nrD}+k_T^0(r)}dV. \tag{7}$$

In these equations, V_{core} is the core volume, σ_A^V is the density of the acceptors per unit of volume, and n_A the number of acceptors per core. Considering the model described in Figure 1, the dV element can be expressed as a function of the solid angle Ω and θ, according to the formula

$$dV = S(r)dr = \Omega r^2 = 2\pi r^2(1-\cos\theta). \tag{8}$$

By the law of cosines

$$r_{core}^2 = r^2 + (r_{core}+e)^2 - 2r(r_{core}+e)\cos\theta, \tag{9}$$

where $r^2{}_{core}$ is the oxide core radius and e the thickness of the polysiloxane shell. Substitution of these expressions gives

$$S(r) = \frac{2\pi r(r-e)(2r_{core}+e-r)}{2r_{core}+e}. \tag{10}$$

By the demonstration in Sec. III C, $k_T^0(r) \ll k_{rD}+k_{nrD}$,

$$\frac{k_T^0(r)}{k_{rD}+k_{nrD}+k_T^0(r)} \approx \frac{k_T^0(r)}{k_{rD}+k_{nrD}}. \tag{11}$$

Finally, k_T and η_T are obtained by integration of Eqs. (6) and (7) between $r = e$ and $r = 2r_{core}+e$, respectively

$$k_T = \frac{R_0^6}{V_{core}\tau_D}\int_e^{2r_{core}+e} \frac{2\pi r(r-e)(2r_{core}+e-r)}{(2r_{core}+e)r^6}dr, \tag{12}$$

$$\eta_T = \frac{R_0^6}{V_{core}\tau_D + (k_{rD}+k_{nrD}}\int_e^{2r_{core}+e} \frac{2\pi r(r-e)(2r_{core}+e-r)}{(2r_{core}+e)r^6}dr, \tag{13}$$

where the integration expression could be denoted by

$$\beta(r_{core}, e) = \int_{e}^{2r_{core}+e} \frac{2\pi r(r-e)(2r_{core}+e-r)}{(2r_{core}+e)r^6} dr. \quad (14)$$

The coefficient β is then correlated to the emitted intensity of sample[57]

$$I_{em} = I_0(1-e^{-\varepsilon cL})\eta_T\Phi_A = \frac{I_0(1-e^{-\varepsilon cL})\Phi_A R_0^6}{V_{core}\tau_D(k_{rD}+k_{nrD})}\beta(r_{core}, e). \quad (15)$$

In this equation, c is the concentration of the pyridine molecules and L the optical length.

The values of I_{em} obtained by the multi-acceptor model were validated by the experimental assays. We elaborated a second series of samples composed of the same core (3.7 nm Eu_2O_3 cores), the same number of pyridine molecules introduced per particle (n = 2.6) but with different thicknesses e varying from 0.28 to 0.71 nm. The europium quantum yield cations Φ_A was found equal to the same value 0.16 (Table I), which confirms that the intensity emitted by the lanthanides after pyridine excitation is effectively proportional to the factor β.

In Figure 7, the coherence between the experimental data and the calculated I_{em} value (by Eq. (15)) demonstrates the validity of the multi-acceptor model for the description of the structures studied. The luminescence intensity of four samples (polysiloxane thicknesses of 0.3 nm, 0.4 nm, 0.6 nm, 0.7 nm) was determined by integrating the emission spectrum in the range between 550 and 640 nm. Time resolved analysis was preferred to steady-state assays to benefit from a baseline reduction: light is collected in a window gate of 5 ms after a delay of 0.1 ms from 270 nm light pulse. All the 670 europium atoms can be directly excited by light pulses. The density of Eu^{3+} ions liable to be sensitized varies with the $1/R^6$ distance from each pyridine molecule as Forster's theory predicted. It is significant that, in the case of $e = 0.3$ nm, the 80% of the total sensitizing effect of a molecule pyridine (the donor) concerns the europium cations (acceptor) that are situated at a distance smaller than 0.7 nm. The rest of the sensitizing contribution (20%) is almost entirely limited to the Eu^{3+} ions that lie at a distance smaller than 1.5 nm from each donor. These results are due to the fact that the Förster distance R_0 (0.89 nm) is of the same order of magnitude than the parameters characteristic of the core/shell geometry ($R_{core} = 1.8$ nm, $e = 0.3$ nm). As the thickness of polysiloxane increases ($e = 0.7$ nm), the influence of the antenna effect on europium atoms changes as expected: the Eu^{3+} ions located at a distance smaller than 1.1 nm contribute to only 60% of the total emission, the other 40% arising from atoms located till a distance of 3.5 nm. These results evidence that the presence of only one antenna per particle would be clearly insufficient to enhance the emission signal of each europium of the core. A more efficient system requires then the presence of multiple donors per particle in order to increase the number of potential europium acceptors (e.g., till 450 pyridine per 0.4 nm thickness shell).

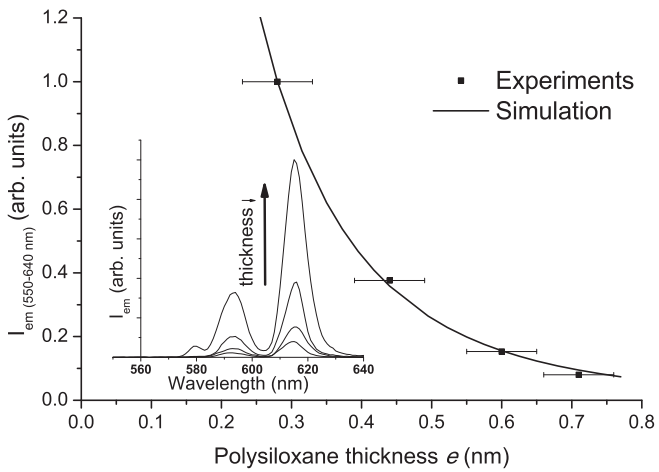

FIG. 7. Comparison between the luminescence intensities of samples measured ($I_{em\,(550\text{–}640nm)}$) integrating the emission spectrum in the range 550–640 nm, and their fit according to the multi-acceptor model. Inset: the emission spectra of the samples differing by their polysiloxane thicknesses.

The value of k_T (achieved in Sec. III C) and the lifetime value of donor τ_D (Table I) allow the calculation of Forster distance R_0 in Eq. (12). R_0 is found equal to 8.9 nm, in consistence with the values found in literature for other donor/acceptor systems such as purely organic ones.[58]

The increase in brightness B is then evaluated comparing the synthesize D/A system studied and the polysiloxane coated europium oxide cores (indicated by subscript A). In the case of a single emitter, the brightness B_A is simply given by the product of the molar extinction coefficient and the emitter quantum yield: $B_A = \varepsilon_A\Phi_A$, whereas the brightness of the D/A system studied (B_{DA}) is $B_{DA} = \varepsilon_D\, D/A\, \eta_T\Phi_A$. Considering the case of sample with shell thickness of 0.44 nm and 400 pyridine molecules grafted per particle, $\frac{B_{DA}}{B_A} = \frac{\varepsilon_D}{\varepsilon_A}\frac{D}{A}\eta_T$ is equal to 375. As expected, this emission enhancement factor is in perfect agreement with the one found experimentally by direct comparison of the luminescence of the adequate D/A system and that of the polysiloxane coated Eu_20_3 cores.

IV. CONCLUSION

We present a new sensitized core-shell nanostructure allowing a significant enhancement of the lanthanides emission. A Eu_2O_3 core (3.7 nm size) is coated by polysiloxane shell with controlled thickness that entraps some amine groups. These functional groups allow further grafting of pyridine molecules onto the particles surface. We experimentally demonstrate that the pyridine molecules act as efficient sensitizers for the europium cations of core. Varying the number of sensitizers per particle, we determined the main optical parameters involved in the lanthanide emission processes. The average transfer efficiency over all the donor-acceptor pairs was calculated as a function of the transfer rate between a single D-A pair; it was found to be independent of the number of sensitizers and equal to 0.14. The radiative and non-radiative decay rates of the donors were also found independent of the number of sensitizers that excludes any self-quenching between pyridine molecules. Moreover, contrary to what happens in macroscopic samples of pure

europium, the nanometric size of oxides preserves quantum yield values closed to 0.12. The donor/acceptor modeling of such system is in complete coherence with the experiments performed on a series of samples varying the thickness of the polysiloxane shell, i.e., the spacing distance between the donors and the acceptors. The treatise helps (i) to explain why the addition of 0.6 pyridines (the antenna) per Eu^{3+} ion allows the enhancing of brightness by a factor 400 and (ii) to illustrate the engineering to carry out performing phosphorescence probes for ultrasensitive detection.

[1]S. W. Hell and J. Wichmann, Opt. Lett. **19**, 780 (1994).
[2]E. Betzig, Science **313**, 1642 (2006).
[3]S. T. Hess, T. P. Girirajan, and M. D. Mason, Biophys. J. **91**, 4258 (2006).
[4]M. J. Rust, M. Bates, and X. Zhuang, Nat. Methods **3**, 793 (2006).
[5]M. Fernandez-Suarez and A. Y. Ting, Nat. Rev. Mol. Cell Biol. **9**, 929 (2008).
[6]F. Wang, W. B. Tan, Y. Zhang, X. Fan, and M. Wang, Nanotechnology **17**, R1 (2006).
[7]J. Lippincott-Schwartz and G. H. Patterson, Methods Cell Biol. **85**, 45 (2008).
[8]K. A. Lukyanov, D. M. Chudakov, S. Lukyanov, and V. V. Verkhusha, Nat. Rev. Mol. Cell Biol. **6**, 885 (2005).
[9]M. Chalfie, Y. Tu, G. Euskirchen, W. W. Ward, and D. C. Prasher, Science **263**, 802 (1994).
[10]E. F. G. Dickson, A. Pollak, and E. P. Diamandis, J. Photochem. Photobiol., B **27**, 3 (1995).
[11]P. G. Sammes and G. Yahioglu, Nat. Prod. Rep. **13**, 1 (1996).
[12]R. Selvin, Nat. Struct. Biol. **7**, 730 (2000).
[13]E. P. Diamandis and T. K. Christopoulos, Anal. Chem. **62**, 1149A (1990).
[14]R. A. Evangelista, A. Pollak, B. Allore, E. F. Templeton, R. C. Morton, and E. P. Diamandis, Clin. Biochem. **21**, 173 (1988).
[15]J. R. Lakowicz, *Principles of Fluorescence Spectroscopy* (Springer, New York, 2006), p. 87.
[16]J. C. G. Bunzli and C. Piguet, Chem. Soc. Rev. **34**, 1048 (2005).
[17]P. Selvin, IEEE J. Sel. Top. Quantum Electron. **2**, 1077 (1996).
[18]B. Alpha, R. Ballardini, V. Balzani, J.-M. Lehn, and N. Sabbatini, Photochem. Photobiol. **52**, 299 (1990).
[19]M. Latvaa, H. Takalob, V. M. Mukkala, C. Matachescu, J. C. Rodriguez-Ubis, and J. Kankare, J. Lumin. **75**, 149 (1997).
[20]E. Brunet, O. Juanes, R. Sedano, and J. C. Rodriguez, Photochem. Photobiol. Sci. **1**, 613 (2002).
[21]M. Xiao and P. R. Selvin, J. Am. Chem. Soc. **123**, 7067 (2001).
[22]Y. W. Yip, H. Wen, W. T. Wong, P. A. Tanner, and K.-L. Wong, Inorg. Chem. **51**, 7013 (2012).
[23]G. M. Jones, C. Wofsy, C. Aurell, and L. A. Sklar, Biophys. J. **76**, 517 (1999).
[24]T. N. Estep and T. E. Thompson, J. Biophys. **26**, 195 (1979).
[25]A. G. Tweet, W. D. Bellamy, and G. L. Gaines, J. Phys. Chem. **41**, 2068 (1964).
[26]P. K. Wolber and B. S. Hudson, J. Biophys. **28**, 197 (1979).
[27]S. Klink, G. Hebbink, L. Grave, F. Peters, F. Van Veggel, D. Reinhoudt, and J. Hofstraat, Eur. J. Org. Chem. **10**, 1923 (2000).
[28]M. Werts, R. Jukes, J. Hofstraat, F. Geurts, and J. Verhoeven, Phys. Chem. Chem. Phys. **4**, 1542 (2002).
[29]F. Lux, A. Mignot, P. Mowat, C. Louis, S. Dufort, C. Bernhard, F. Denat, F. Boschetti, C. Brunet, R. Antoine, P. Dugourd, S. Laurent, L. V. Elst, R. Muller, L. Sancey, V. Josserand, J. L. Coll, V. Stupar, E. Barbier, C. Remy, A. Broisat, C. Ghezzi, G. Le Duc, S. Roux, P. Perriat, and O. Tillement, Angew. Chem., Int. Ed. **50**, 12299 (2011).
[30]A. Mignot, C. Truillet, F. Lux, L. Sancey, C. Louis, F. Denat, F. Boschetti, L. Bocher, A. Gloter, O. Stéphan, R. Antoine, P. Dugourd, D. Luneau, G. Novitchi, L. C. Figueiredo, P. C. de Morais, L. Bonneviot, B. Albela, F. Ribot, L. Van Lokeren, I. Déchamps-Olivier, F. Chuburu, G. Lemercier, C. Villiers, P. N. Marche, G. Le Duc, S. Roux, O. Tillement, and P. Perriat, Chem. Eur. J. **19**, 6122 (2013).
[31]M. Ou, B. Mutelet, M. Martini, R. Bazzi, S. Roux, G. Ledoux, O. Tillement, and P. Perriat, J. Colloid Interface Sci. **333**, 684 (2009).
[32]C. Louis, R. Bazzi, C. A. Marquette, J. L. Bridot, S. Roux, G. Ledoux, B. Mercier, L. Blum, P. Perriat, and O. Tillement, Chem. Mater. **17**, 1673 (2005).
[33]J. L. Bridot, A. C. Faure, S. Laurent, C. Rivière, C. Billotey, B. Hiba, M. Janier, V. Josserand, J. L. Coll, L. V. Elst, R. Muller, S. Roux, P. Perriat, and O. Tillement, J. Am. Chem. Soc. **129**, 5076 (2007).
[34]See supplementary material http://dx.doi.org/10.1063/1.4821428 for details about synthesis, characterization, and modelization of the core-shell particles.
[35]J. M. Senegas, G. Bernardinelli, D. Imbert, J. C. G. Bünzli, P. Y. Morgantini, J. Weber, and C. Piguet, Inorg. Chem. **42**, 4680 (2003).
[36]G. Blasse and B. C. Grabmaier, *Luminescent Materials* (Springer-Verlag, New York, 1994).
[37]K. Binnemans, Chem. Rev. **109**, 4283 (2009).
[38]D. L. Dexter, J. Chem. Phys. **21**, 836 (1953).
[39]R. M. Clegg, Lab. Tech. Biochem. Mol. Biol. **33**, 1 (2009).
[40]A. Huignard, V. Buissette, A. C. Franville, T. Gacoin, and J. P. Boilot, J. Phys. Chem. B **107**, 6754 (2003).
[41]B. Mercier, C. Dujardin, G. Ledoux, C. Louis, and O. Tillement, J. Appl. Phys. **96**, 650 (2004).
[42]Y. Wang, X. Guo, T. Endo, Y. Murakami, and M. Ushirozawac, J. Solid State Chem. **177**, 2242 (2004).
[43]J. C. Krupa, J. Alloys Compd. **225**, 1 (1995).
[44]C. Louis, S. Roux, G. Ledoux, C. Dujardin, O. Tillement, B. L. Cheng, and P. Perriat, Chem. Phys. Lett. **429**, 157 (2006).
[45]E. Nakazawa and F. Shiga, J. Lumin. **15**, 255 (1977).
[46]E. Nakazawa, J. Lumin. **100**, 89 (2002).
[47]W. F. Sager, N. Filipescu, and F. A. Serafin, J. Phys. Chem. **69**, 1092 (1965).
[48]O. L. Malta, J. Lumin. **71**, 229 (1997).
[49]N. M. Shavaleev, F. Gumy, R. Scopelliti, and J. C. G. Bünzli, Inorg. Chem. **48**, 5611 (2009).
[50]M. Kleinerman, J. Chem. Phys. **51**, 2370 (1969).
[51]A. R. Williams and S. A. Winfield, Analyst **108**, 1067 (1983).
[52]M. Martini, P. Perriat, M. Montagna, R. Pansu, C. Julien, O. Tillement, and S. Roux, J. Phys. Chem. C **113**, 17669 (2009).
[53]B. Mutelet, P. Perriat, G. Ledoux, D. Amans, F. Lux, O. Tillement, C. Billotey, M. Janier, C. Villiers, R. Bazzi, S. Roux, G. Lu, Q. Gong, and M. Martini, J. Appl. Phys. **110**, 094317 (2011).
[54]G. A. Crosby, E. Whan, and J. J. Freeman, J. Phys. Chem. **66**, 2493 (1962).
[55]E. R. Clark, J. R. Darwent, B. Demirci, K. Flunder, A. F. Gaines, and A. C. Jones, Energy Fuel **1**, 392 (1987).
[56]B. K. Fung and L. Stryer, Biochemistry **17**, 5241 (1978).
[57]Y. Ma and Y. Wang, Coord. Chem. Rev. **254**, 972 (2010).
[58]R. M. Clegg, A. Murchie, A. Zechel, and D. M. J. Lilley, Proc. Natl. Acad. Sci. U.S.A. **90**, 2994 (1993).